travened by Dworin's analysis of the heirarchy of equations of motion for Anderson's model.[24] He derived an integral equation for G_d bearing a resemblance to the integral equation occurring in the aforementioned treatment of the *s-d* exchange model.[16] However, the key integral operator is not singular, but broadened by a finite imaginary term which could correspond to our T_s. Dworin estimates that this term is of *the same* order as the Kondo temperature.

The other major criticism which can be leveled against the RRPA on the basis of equation-of-motion calculations is its failure to produce a spectral density with peaks at ϵ_d and ϵ_d+U.[24,25] The RRPA simulates this structure only to the extent that the spectral density is spread over a range of order U. It is not clear to what extent the details of the spectrum at large energy effect the low-energy structure associated with the Kondo effect.

ACKNOWLEDGMENTS

The author acknowledges stimulating discussions with H. Suhl, W. F. Brinkman, J. A. Appelbaum, M. Levine, and R. A. Weiner.

[24] L. Dworin, Phys. Rev. **164**, 841 (1967).

[25] B. Kjöllerström, D. J. Scalapino, and J. R. Schrieffer, Bull. Am. Phys. Soc. **11**, 79 (1966).

PHYSICAL REVIEW VOLUME 186, NUMBER 2 10 OCTOBER 1969

Magnetic Neutron Scattering in Dysprosium Aluminum Garnet. I. Long-Range Order*

J. C. NORVELL† AND W. P. WOLF
Yale University, New Haven, Connecticut 06511

AND

L. M. CORLISS, J. M. HASTINGS, AND R. NATHANS
Brookhaven National Laboratory, Upton, New York 11973

(Received 5 May 1969)

Magnetic long-range order has been studied in antiferromagnetic dysprosium aluminum garnet (DAG) using coherent neutron scattering to measure the sublattice magnetization in the vicinity of the critical temperature. The value of the critical exponent β in the power-law expression for the magnetization $M \sim(\Delta T)^\beta$ was found to be 0.26 ± 0.02 for the temperature range $0.0010<\Delta T_c<0.056$. This is significantly lower than the theoretical estimate of 0.312 for the three-dimensional nearest-neighbor Ising model, with which DAG is compared.

I. INTRODUCTION

THERE has recently been much interest in the study of the order-disorder phenomena that occur in magnetic systems at the critical point T_c.[1,2] In antiferromagnetics the long-range order of atomic spins that appears for $T<T_c$ gives rise to a spontaneous sublattice magnetization M, the appropriate order parameter for magnetic systems. As the temperature increases towards T_c, the long-range order decreases and vanishes at T_c, and thus the spontaneous sublattice magnetization approaches zero. The temperature dependence is characterized by the critical exponent β, which is defined[1] by

$$M \propto [(T_c-T)/T_c]^\beta \quad \text{as } T\rightarrow T_c. \tag{1}$$

The present paper (I) describes the determination of β from measurements of the magnetization below the critical point. The following paper (II) [Phys. Rev., **186**, 567 (1969)] describes the critical scattering above T_c and the evaluation of the relevant parameters γ, ν, and η.

The techniques of neutron diffraction provide an excellent tool for the investigation of these magnetic order-disorder phase transitions. The spontaneous sublattice magnetization gives rise to strong magnetic Bragg peaks that occur at reciprocal-lattice points, and thus can be rather easily measured. The scattering cross section for such a reflection is proportional to M^2 and thus 2β can be determined from a study of the temperature dependence of the intensity. Diffuse critical scattering is superimposed on these Bragg peaks, but this scattering is relatively weak except in the temperature region very close to the critical point. At lower temperatures the main difficulty in determining β is ensuring that extinction does not affect the results.

Theoretical estimates of the critical exponent β have been obtained from numerous statistical-mechanical

* Work performed under the auspices of the U. S. Atomic Energy Commission.

† Present address: Los Alamos Scientific Laboratory, Los Alamos, N. M.

[1] See, e.g., C. Domb, Advan. Phys. **9**, 149 (1960); M. E. Fisher, Rept. Progr. Phys. **30**, 615 (1967).

[2] P. Heller, Rept. Progr. Phys. **30**, 731 (1966).

calculations. Effective field theories and all finite cluster models predict $\beta=\frac{1}{2}$, in clear disagreement with experimental results on most real systems, which seem to have β values closer to $\frac{1}{3}$. Recent numerical calculations for simple models, however, have yielded better results. Work on one of these, the Ising model, has been particularly extensive. The use of Padé-approximant methods in low-temperature expansions for three-dimensional Ising models with short-range forces has lead to precise estimates of β, as well as other critical exponents.[3–5] The most recent investigations of Baker and Gaunt[5] give

$$\beta=0.312_{-0.005}{}^{+0.002}$$

for simple, bcc, and fcc lattices. Thus β appears to be independent of the detailed structure of the model.

Although few Ising-like systems are found in nature, several new magnetic materials with very anisotropic magnetic properties have recently become available for study. Among these is dysprosium aluminum garnet (DAG), which has been shown to be an extremely good approximation to an Ising antiferromagnet. The experimental determination of the critical exponents for this material is thus of considerable interest.

II. DAG AS AN ISING ANTIFERROMAGNET

In order to compare the experimental results with theoretical calculations on Ising models, it is important to know how closely DAG actually conforms to these models, All Ising model calculations start from an interaction Hamiltonian of the form

$$\mathcal{H}=\sum_{i>j} J(\mathbf{r}_{ij})S_{zi}S_{zj}, \tag{2}$$

which has the important property that all its terms commute. The interacting spins are usually restricted to the case $S=\frac{1}{2}$, so that

$$S_{zi}=\pm\tfrac{1}{2}, \tag{3}$$

though the extension to the general case of $S>\frac{1}{2}$ can be achieved at the expense of some complication.[1] The interaction parameters $J(\mathbf{r}_{ij})$ are generally assumed to be short-ranged, and most detailed calculations to date have only considered the case

$$\begin{aligned} J(\mathbf{r}_{ij})&=J, \quad i,\ j=\text{nearest neighbors}\\ &=0, \qquad =\text{other neighbors}. \end{aligned} \tag{4}$$

The fourth ingredient in all calculations is the choice of a lattice. For three-dimensional cubic systems in particular, only the simple, bcc, and fcc arrangements have been studied,[1] but there is good reason to believe that the details of the coordination are unimportant in the critical region.[1] As we shall see, only the restriction of Eq. (4) will in fact provide an significant difference from the situation in DAG, and even there the approximation is quite good.

DAG ($Dy_3Al_5O_{12}$) has the garnet crystal structure, with eight molecules in the unit cell. The structure belongs to the space group $Ia3d(O_h{}^{10})$ with $a_0=12.04$ Å.[6] There are 24 Dy^{3+} ions on the (c) sites of the unit cell. The point symmetry is D_2 and a strong crystal field splits the ground state ${}^6H_{15/2}$ of each Dy^{3+} ion into a series of eight Kramer doublets. Magnetic-susceptibility[7,8] and specific-heat[9] measurements have shown that the ground-state doublet lies well below the first excited state, and recent optical measurements[10,11] have given the splitting as 70 cm^{-1} ($\sim$100°K). DAG orders antiferromagnetically at 2.5°K,[8,9] and in this region one may therefore neglect the excited states to a very good approximation and represent each Dy^{3+} ion by an effective spin $S'=\frac{1}{2}$.

The nature of the ground-state doublet has been inferred from a series of paramagnetic-resonance,[7] magnetization,[8,12–14] and optical measurements,[10,11] which all show it to be highly anisotropic, composed mainly of $|J_z=\pm\frac{15}{2}\rangle$, where z is the local D_2 axis which is parallel to one of the principal cubic axes.[15] The magnetic g tensor corresponding to a pure $|\pm\frac{15}{2}\rangle$ state would have principal values $g_x=g_y=0$, $g_z=20$, in close agreement with the experimental estimates $g_x\approx g_y\lesssim 1$, $g_z=18.2\pm0.2$.

If we neglect the small admixtures of states with $J_z\neq\pm\frac{15}{2}$, we can immediately show that only Ising interactions of the form of Eq. (2) can act between the effective spins describing the ions in their ground states. This is because any off-diagonal term between the effective spins would have to correspond to a real interaction coupling states with $\Delta J_z=\pm15$, whereas the maximum ΔJ_z for any interaction involving pairs of f electrons is 7 ($=2l+1$).

---

[3] G. A. Baker, Jr., Phys. Rev. **124**, 768 (1961).
[4] J. W. Essam and M. E. Fisher, J. Chem. Phys. **38**, 802 (1963).
[5] G. A. Baker, Jr., and D. S. Gaunt, Phys. Rev. **155**, 545 (1967).

[6] E. Bertaut and F. Forrat, Compt. Rend. **243**, 1219 (1956); S. Geller and M. A. Gilleo, Acta Cryst. **10**, 239 (1957).
[7] M. Ball, M. T. Hutchings, M. J. M. Leask, and W. P. Wolf, in *Proceedings of the Eighth International Conference on Low-Temperature Physics, 1962*, edited by R. O. Davies (Butterworths Scientific Publications, Ltd., London, 1963), p. 248.
[8] A. F. G. Wyatt, Ph.D. thesis, Oxford University, 1963 (unpublished).
[9] M. Ball, M. J. M. Leask, W. P. Wolf, and A. F. G. Wyatt, J. Appl. Phys. **34**, 1104 (1963).
[10] K. A. Gehring (private communication).
[11] P. Grünberg, S. Hüfner, E. Orlick, and J. Schmitt, Phys. Rev. **184**, 285 (1969).
[12] M. Ball, W. P. Wolf, and A. F. G. Wyatt, Phys. Letters **10**, 7 (1964).
[13] B. Schneider, B. E. Keen, D. P. Landau, and W. P. Wolf (unpublished).
[14] W. P. Wolf, in *Proceedings of the International Conference on Magnetism, Nottingham, 1964* (The Institute of Physics and the Physical Society, London, 1964), p. 555.
[15] It is convenient to choose a set of *local* axes at each site to correspond to the local D_2 symmetry, and to express all effective-spin operators for any particular ion relative to these axes (see, for example, Ref. 13). The z axes at two different sites will therefore not necessarily be parallel in real space, though the corresponding term in an Ising-model Hamiltonian $S_{zi}S_{zj}$ will still be diagonal relative to a representation $|S_{zi}S_{zj}\rangle$.

TABLE I. Interactions in DAG.

Order of neighbor j	No. of neighbors n_j	Distance from origin r_{0j} (Å)	Dipole interaction energy per pair[a,b]	Nondipolar energy per pair[a–c]	Contribution to energy[a] at $T=0$°K from n_j neighbors	Spin orientation of neighbors (origin spin in $-z$ direction)	Nearest-neighbor subset
1	4	3.69	−17.42	−9.06	−105.90	$(\pm x,\pm y)$	a
2	8	5.63	−6.28	+0.82	−43.73	$2(\pm x,\pm y)$	b
3	2	6.02	+16.00	−2.24	+27.52	$2(+z)$	b
4	8	6.73	±2.29		0	$4(\pm z)$	$(4a)$ $(4b)$
5	4	7.06	+6.09		−24.36	$(\pm x,\pm y)$	a
6	8	8.24	+1.56		+12.46	$2(\pm x,\pm y)$	b
7	4	8.51	−2.83		−11.31	$4(+z)$	b
				Total for 38*nn*	−145.32		
				Total for all neighbors[d]	−130.30		

[a] In units $g_z^2\mu_B^2/4k_Ba_0^3 \approx 0.029$°K.
[b] Signs relative to the observed ordered state at $T=0$°K.
[c] After Ref. 20.
[d] Infinite dipole sum plus estimated nondipolar contributions, after Ref. 20.

The small admixtures produced by the nonaxial components in the crystal field will allow effective-spin interactions of the form $S_{xi}'S_{zj}'$ and $S_{xi}'S_{xj}'$, but these can be shown to be relatively small. In particular, for magnetic dipole interactions, which constitute the major part of the diagonal interactions, terms of the form $S_{xi}'S_{zj}'$ will be reduced by a factor of the order of $g_x/g_z \sim 1/18$ relative to the $S_{zi}'S_{zj}'$ term, while $S_{xi}'S_{xj}'$ terms are reduced by factors of the order of $(g_x/g_z)^2 \sim (1/18)^2$. Moreover, measurements of the metamagnetic transitions produced by applied magnetic fields at very low temperatures[12,16,17] have shown no evidence of any spin-flop phase, such as would be stable in fields just above the transition if the interactions were not predominantly Ising-like in the sense of Eq. (2).

The range of the effective interaction has been estimated from several measurements of the low-temperature specific-heat[9] and susceptibility[8,13] measurements, optical spectra,[18] and the angular dependence of the critical field for the metamagnetic transition.[17–19] The analysis[17,20] shows that the interactions are primarily due to magnetic dipole coupling, with a small but significant nondipolar contribution to the nearest-neighbor interaction and only very small contributions to the more distant neighbor interactions. Estimates for the interaction energies are given in Table I. It can be seen that the nearest-neighbor interaction is clearly dominant, but that the interactions with second and third nearest neighbors are not really negligible, even though they tend to cancel in the ordered state. No detailed calculations have been made for a situation as complex as this, but calculations on various Ising models with different numbers of interacting *near* neighbors have shown that the critical indices are essentially independent of the details of the coordination.[1] It seems quite unlikely, therefore, that the nonzero *near*-neighbor interactions would alter the critical-point behavior in any significant way.

On the other hand, the effect of the many very weak interactions between the more distant neighbors is very difficult to assess, and it is this particular difference from the theoretical Ising models which could possibly lead to significant *qualitative* discrepancies. Extension of the theory to include long-range interactions is unfortunately very difficult, and at the present time we can only speculate that the antiferromagnetic correlations produced by the stronger near-neighbor interactions will tend to produce a cancellation of the many long-range terms. We shall consider this point again in the light of our experimental results.

The ordered antiferromagnetic state of DAG is complex. It is dominated by the extreme anisotropy which constrains each magnetic moment to its own local z axis in an arrangement which has the full cubic symmetry even in the antiferromagnetic state. The spin arrangement was predicted on the basis of resonance and susceptibility measurements[7] and it was subsequently verified by neutron diffraction studies on DAG powder samples.[21,22] Figure 1 shows the magnetic unit cell, which is identical with the chemical cell. It may be seen that the magnetic environment of every spin is the same relative to its local z axis, and that the structure can be described in terms of three identical interpenetrating antiferromagnetic substructures, in each of which the spins are collinear and directed along one of the cube edges. The relative orientations of the

[16] B. E. Keen, D. P. Landau, B. Schneider, and W. P. Wolf, J. Appl. Phys. **37**, 1120 (1966).
[17] R. Bidaux, P. Carrara, and B. Vivet (unpublished).
[18] A. H. Cooke, K. A. Gehring, M. J. M. Leask, D. Smith, and J. H. M. Thornley, Phys. Rev. Letters **14**, 685 (1965).
[19] B. E. Keen, D. P. Landau, and W. P. Wolf, Phys. Letters **23**, 202 (1966).
[20] B. Schneider, D. P. Landau, B. E. Keen, and W. P. Wolf, Phys. Letters **23**, 210 (1966).
[21] A. Herpin and P. Mériel, Compt. Rend. **259**, 2416 (1964).
[22] J. M. Hastings, L. M. Corliss, and C. G. Windsor, Phys. Rev. **138A**, 176 (1965).

different spins in the unit cell are given in Table II, together with a number indicating the order in distance of the neighbor relative to the spin at $(\frac{1}{2},\frac{1}{4},\frac{3}{8})$ taken as origin. The corresponding orientations of the first seven shells of neighbors are given in Table I.

One may also subdivide the Dy^{3+} sites into two subsets (denoted by *a* and *b* in the last column of Tables I and II), each composed of ions connected by nearest-neighbor paths. The two subsets are coupled by second- and third-nearest-neighbor interactions and the establishment of long-range order thus depends in an essential way on other than nearest-neighbor interactions. However, these complications are almost certainly unimportant in the critical region where, as we shall show, correlations extend to many hundreds of near neighbors, so that the details of the near-neighbor interactions will almost certainly be averaged out. The subdivision into *a* and *b* subsets will become useful in the formulation of the critical scattering cross section (see II), although we shall again be forced to reduce the expressions to an average over all the spin correlations.

One additional possible complication which must be considered is the large hyperfine interaction which exists in DAG.[8] The dominant term has the form $A_z S_z' I_z$, with $A_z \approx 0.07°K$, which is quite comparable with the other interactions. Fortunately, it is possible to show,[23] by means of an exact factorization of the partition function, that the effect of this term does not alter the critical-point behavior of *any* Ising-like system described by Eq. (2). However, there are also smaller terms of the form $A_x S_x' I_x$, which are reduced in proportion to g_x/g_z, and the effect of these has not been discussed theoretically. One may speculate that these are single-ion interactions which cannot affect the growth of long-range correlations in any significant way, but there is no rigorous proof of this idea. Fortunately, the high anisotropy of the *g* tensor makes the noncommuting terms very small, so that even if there were an effect, it would probably be important only very close to the critical point.

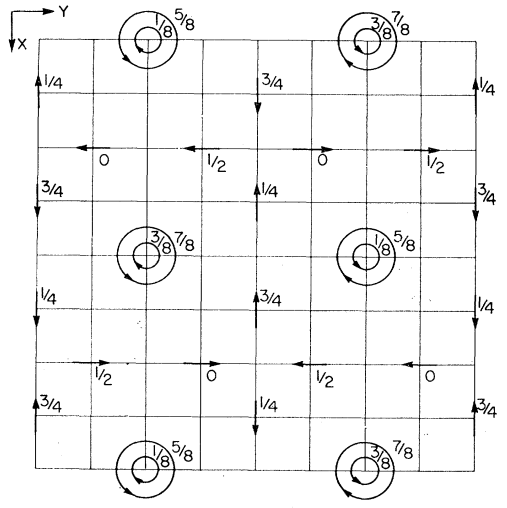

FIG. 1. Spin arrangement in DAG. Dy^{+3} ions are in special positions 24(*c*) of space group *Ia3d*. The numbers in the figure give the height above the $z=0$ plane. Spins pointing along the positive *z* axis are indicated as current loops in a right-hand sense.

[23] D. C. Mattis and W. P. Wolf, Phys. Rev. Letters **16**, 899 (1966).

TABLE II. Atomic positions and spin orientations in DAG.

Dy^{+3} Position	Order of neighbor relative to spin at $(\frac{1}{2},\frac{1}{4},\frac{3}{8})$	Spin direction	Type
$(\frac{1}{8},0,\frac{1}{4})$	2	$-x$	*b*
$(\frac{1}{4},\frac{1}{8},0)$	2	$-y$	*b*
$(0,\frac{1}{4},\frac{1}{8})$	4	$-z$	*b*
$(\frac{3}{8},0,\frac{3}{4})$	2	$+x$	*b*
$(\frac{3}{4},\frac{3}{8},0)$	2	$+y$	*b*
$(0,\frac{3}{4},\frac{3}{8})$	7	$+z$	*b*
$(\frac{5}{8},0,\frac{1}{4})$	1	$+x$	*a*
$(\frac{1}{4},\frac{5}{8},0)$	5	$+y$	*a*
$(0,\frac{1}{4},\frac{5}{8})$	4	$+z$	*a*
$(\frac{7}{8},0,\frac{3}{4})$	5	$-x$	*a*
$(\frac{3}{4},\frac{7}{8},0)$	8	$-y$	*a*
$(0,\frac{3}{4},\frac{7}{8})$	10	$-z$	*a*
$(\frac{5}{8},\frac{1}{2},\frac{3}{4})$	2	$-x$	*b*
$(\frac{3}{4},\frac{5}{8},\frac{1}{2})$	2	$-y$	*b*
$(\frac{1}{2},\frac{3}{4},\frac{5}{8})$	4	$-z$	*b*
$(\frac{7}{8},\frac{1}{2},\frac{1}{4})$	2	$+x$	*b*
$(\frac{1}{4},\frac{7}{8},\frac{1}{2})$	6	$+y$	*b*
$(\frac{1}{2},\frac{1}{4},\frac{7}{8})$	3	$+z$	*b*
$(\frac{1}{8},\frac{1}{2},\frac{3}{4})$	5	$+x$	*a*
$(\frac{3}{4},\frac{1}{8},\frac{1}{2})$	1	$+y$	*a*
$(\frac{1}{2},\frac{3}{4},\frac{1}{8})$	4	$+z$	*a*
$(\frac{3}{8},\frac{1}{2},\frac{1}{4})$	1	$-x$	*a*
$(\frac{1}{4},\frac{3}{8},\frac{1}{2})$	1	$-y$	*a*
$(\frac{1}{2},\frac{1}{4},\frac{3}{8})$	0	$-z$	*a*

We can conclude from all this that DAG will generally be a very good approximation to the usual theoretical Ising models, with the one reservation that the weak long-range magnetic dipole interactions might perhaps modify the detailed behavior in the critical region.

III. EXPERIMENTAL PROCEDURE

The present experiment was performed on a two-crystal diffractometer using the experimental arrangement shown in Fig. 2.[24] The monochromator was a germanium crystal reflecting from (111) in transmission geometry. This choice of reflection minimized beam contamination from $\frac{1}{2}\lambda$ neutrons. A wavelength of 1.309 Å was used throughout. In order to increase the available intensity the germanium crystal was plastically deformed so that its mosaic spread was increased from seconds of arc to 14 ft. This procedure unfortunately resulted in a non-Gaussian mosaic distribution, but the effect of this was automatically included in the measured resolution function. The

[24] A more complete description of the experimental details is given in J. C. Norvell, Ph.D. thesis, Yale University, 1968 (unpublished).

collimation consisted of a 10-ft horizontal in-pile collimator, a 10-ft vertical monochromator-to-sample collimator, and 14-ft horizontal and 14-ft vertical collimators in front of the counter. Although good instrumental collimation is not important in the measurement of coherent scattering, it is helpful in decreasing the critical scattering contribution to the background near T_c.

The DAG sample was a single crystal in the shape of a disk with a diameter of 1.7 cm and a thickness of 0.164 cm. The crystal was cut with (110) faces from a large boule that had been pulled from the melt and then ground smooth. X-ray Laue back-reflection photographs verified the orientation to less than 0.5°, and indicated no twinning. The neutron rocking curve of the DAG (440) nuclear peak is shown in Fig. 3 and indicates a width at half-height $\Delta w = 1.8$ ft. Making the appropriate resolution corrections, the mosaic spread was found to be 1.6 ft. This observed mosaic spread is very small compared to other parameters and caused no broadening of the resolution function.

A sample holder containing the crystal, a thermometer, and a heater was constructed from a single crystal of aluminum, so oriented as to avoid interfering reflections (Fig. 4). The sample, surrounded by a phosphor bronze spring, was placed in a vertical slot of the sample holder and locked in place by an aluminum tongue. The spring provided some thermal contact between the DAG sample and the surrounding aluminum and maintained a fixed orientation. Cd was used to shield the top and bottom of the sample holder from the neutron beam.

The sample temperature was measured with a calibrated germanium thermometer. In the region of 2.5°K, the resistance of the thermometer was almost 3500 Ω, dR/dT was about 3.5 Ω/m°K, and temperatures were measured to 0.1 m°K on a relative scale. The thermometer was wrapped in aluminum foil, coated with Apiezon N grease to provide thermal contact, and then slipped inside the hole provided for it. Small temperature gradients between the sample and the thermometer were unimportant since only relative temperatures were required.

The whole sample holder assembly was contained

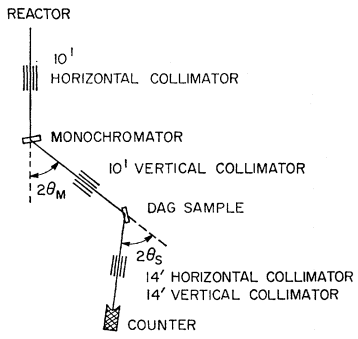

FIG. 2. Experimental arrangement, showing placement of Soller-slit collimators.

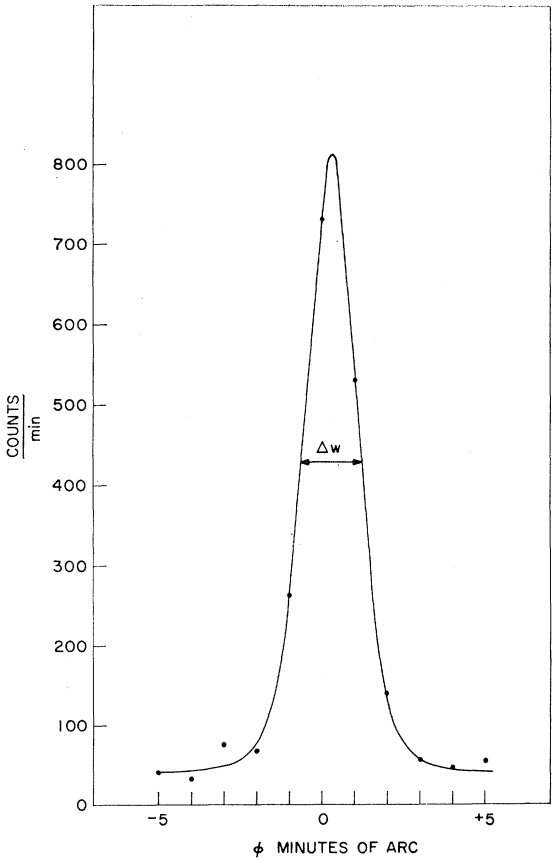

FIG. 3. (440) rocking curve of sample crystal. Full width at half-maximum is 1.6 ft after correction for instrumental resolution.

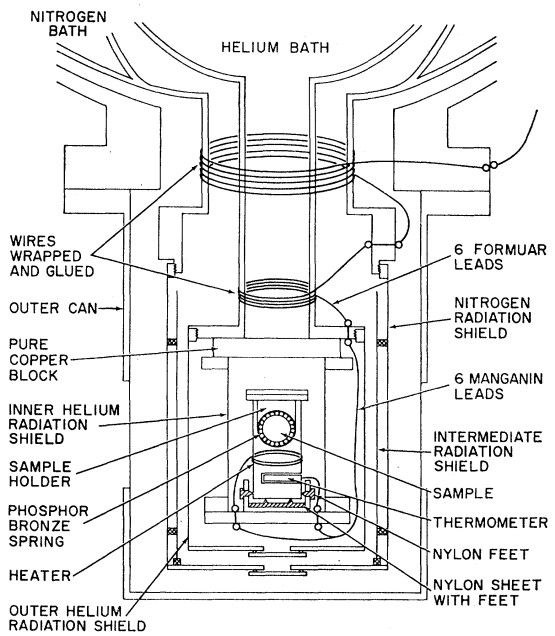

FIG. 4. Lower section of helium cryostat.

in a Linde LNI-54 12-liter helium Dewar fitted with several radiation shields and a heater. The Dewar tail section is shown in Fig. 4. The sample holder was isolated and supported by Nylon feet. The four radiation shields were made of 0.010-in. Al. Since the temperature had to be maintained constant to less than 1 mdeg over long counting periods, a two-step temperature control process was used. The helium-bath temperature was maintained constant to less than 2 m°K at about 2.0°K by a vapor-pressure regulator. The heater attached directly to the sample holder was controlled separately by an electronic temperature controller using proportional, integral, and rate amplifiers. The effectiveness of the temperature control was evaluated by observing the (330) Bragg magnetic peak close to T_c, where the intensity varies rapidly with temperature. These measurements showed that ~5 h were required for the sample to reach thermal equilibrium at a given temperature and that the temperature was then maintained constant to within 0.2 m°K for up to 80 h. In all of our measurements, at least 8 h were allowed for the system to equilibrate. The possibility of a temperature gradient across the sample was also investigated. Using a cadmium slit system, the Bragg magnetic peak intensity was measured at the top and bottom of the sample. These measurements indicated the absence of temperature gradients larger than about 0.3 m°K.

IV. MEASUREMENTS AND CORRECTIONS

The spontaneous sublattice magnetization is obtained from the intensities of the magnetic Bragg reflections.

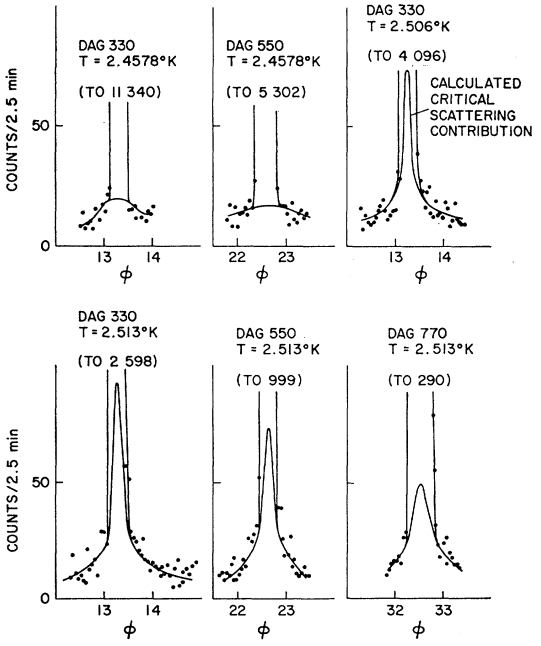

FIG. 5. Representative 2:1 scans of the Bragg magnetic peaks showing critical scattering in the wings and extrapolations to the region of Bragg scattering as explained in the text.

The (330), (550), and (770) peaks were measured at 14 different temperatures from 2.3780 to 2.5149°K. The measurements were taken in a random order to avoid systematic errors. These three peaks were chosen because their relative intensities at any given temperature were sufficiently different, their nuclear structure factors were zero (although small multiple-Bragg peaks were found), and they were easily accessible by changing only the sample table angle (φ) and counter angle (2θ). At each temperature, at least 16 h, i.e., three times the minimum, were allowed for the sample to equilibrate. The integrated intensity of each peak was measured by a 2:1 scan. Since the values of the resolution function changed rapidly in reciprocal space, even small displacements made in filling the Dewar moved the crystal and hence the position of the Bragg peak measurably with respect to the resolution function, thus altering slightly the integrated intensity. Coarse collimation would have removed this difficulty, but, as mentioned previously, this would have greatly increased the critical scattering background. As a result, the proportionality constant in the power law for a particular reflection varied slightly from one filling to another and had to be normalized in the final analysis. The data collected for a given helium filling are designated as a "run," which consists of a set of intensities obtained for all three Bragg peaks at several temperatures.

Weak multiple-Bragg nuclear peaks were found at each of the three magnetic reciprocal-lattice points. They were measured before each run at 4.2°K, where the magnetic scattering is negligible, and subtracted from the magnetic Bragg peaks. These corrections amounted to only about 2% at $T=2.515$°K and decreased rapidly at lower temperatures.

The critical scattering background was estimated by examining the scattering outside the region of the Bragg peak. This region was determined at low temperatures where accurate estimates of the base width of the coherent scattering could be made. The scattering that falls outside these regions was assumed to be entirely critical scattering. Figure 5 shows the base of six of the 2:1 scans. Assuming Lorentzian behavior for the critical scattering cross section, the scattering in the wings of (330) φ scans (see II) was used to predict the critical scattering at the reciprocal-lattice point. This peak height, which is identical for the φ scan and the 2:1 scan, was then joined smoothly to the observed wings of the 2:1 scans. For one case, the convolution was performed for the entire angular range of a 2:1 scan and good agreement was obtained with the observed scattering in the wings as shown for the (330) scan at $T=2.506$°K in Fig. 5. The integral of the critical scattering curve in the region of overlap with the Bragg peak was then evaluated and used as the background, B_{cs}. For the (550) and (770) peaks, the value of the critical scattering was estimated by reducing the (330) critical scattering at each reciprocal-

TABLE III. Observed intensities, weighting factors for data analysis, and derived normalization constants.

(*hh*0)	T	$1-T/T_c$ (T_c=2.5175°K)	Run	$I_{corr}=I_T-B_{cs}$	$\epsilon=(I_T)^{1/2}+\frac{1}{2}B_{cs}$	B_{cs}/I_{corr}	$\ln A_i^h$ [a]
(330)	2.5100	0.00298	1	8 859	486	0.089	$\ln A_1^3=11.63$
	2.4579	0.02367		25 772	357	0.015	
	2.4851	0.01287	2	16 396	370	0.029	$\ln A_2^3=11.48$
	2.5010	0.00655		10 927	392	0.052	
	2.5060	0.00457		9 082	419	0.070	
	2.5130	0.00179		5 773	491	0.142	
	2.4950	0.00894	3	16 050	394	0.033	$\ln A_3^3=11.71$
	2.4680	0.01966		25 643	361	0.016	
	2.4330	0.03357		33 699	349	0.0098	
	2.3780	0.05541		43 191	359	0.0069	
	2.5149	0.00103	4	5 989	513	0.144	$\ln A_4^3=11.71$
	2.4180	0.03952		36 149	349	0.0087	
	2.4780	0.01569		22 624	377	0.020	
	2.5030	0.00576		13 662	424	0.045	
(550)	2.5100	0.00298	1	5 799	340	0.045	$\ln A_1^5=11.30$
	2.4579	0.02367		18 595	302	0.0089	
	2.4851	0.01287	2	9 469	299	0.021	$\ln A_2^5=10.95$
	2.5010	0.00655		6 550	359	0.042	
	2.5060	0.00457		5 431	327	0.046	
	2.5130	0.00179		3 389	373	0.110	
	2.4950	0.00894	3	11 265	323	0.019	$\ln A_3^5=11.36$
	2.4680	0.01966		18 617	307	0.0091	
	2.4330	0.03357		23 797	300	0.0061	
	2.3780	0.05541		30 202	310	0.0045	
	2.5149	0.00103	4	4 112	394	0.079	$\ln A_4^5=11.39$
	2.4180	0.03952		26 437	353	0.0072	
	2.4780	0.01569		16 414	320	0.012	
	2.5030	0.00576		9 607	340	0.025	
(770)	2.5100	0.00298	1	3 863	306	0.062	$\ln A_1^7=10.94$
	2.4579	0.02367		13 039	265	0.012	
	2.4851	0.01287	2	5 620	247	0.030	$\ln A_2^7=10.42$
	2.5010	0.00655		3 919	255	0.048	
	2.5060	0.00457		3 134	274	0.069	
	2.5130	0.00179		1 974	304	0.129	
	2.4950	0.00894	3	6 945	264	0.026	$\ln A_3^7=10.90$
	2.4680	0.01966		11 339	262	0.014	
	2.4330	0.03357		15 050	264	0.0093	
	2.3780	0.05541		19 298	275	0.0070	
	2.5149	0.00103	4	2 562	315	0.101	$\ln A_4^7=10.93$
	2.4180	0.03952		16 705	265	0.0081	
	2.4780	0.01569		10 531	264	0.015	
	2.5030	0.00576		5 781	283	0.035	

[a] Values determined by least-squares fit using all scans and $T_c=2.5175$°K, as discussed in the text.

lattice point by the magnetic form factor f^2 plus an additional 10 and 20%, respectively, to allow for the reduction in scattering caused by the broadening of the resolution function. The critical scattering curves were then drawn in with the assistance of the wings and integrated. Values of B_{cs} estimated in the above manner are given in Table III. These corrections were small in all but a few cases, averaging about 6% with a maximum of 14%. They were accurate to about 20%. The scans with relatively large corrections were assigned small weights in the final least-squares fitting.

It is important in these measurements to ensure that the intensities are not affected by extinction, which, if present, would reduce the stronger intensities more than the weak ones and thus spoil the simple relation between sublattice magnetization and intensity. Since β measures the increase in intensity with decrease in temperature, the presence of extinction would lead to an erroneously low value. Extinction in the DAG sample was studied by an examination of numerous nuclear reflections. The ratio of calculated to observed intensities showed no trend with intensity, indicating the absence of extinction. There were, however, some discrepancies in these ratios which appear to be related to the fact that the surface had been ground while the interior was more perfect. The poorest agreement was found between intensities measured in "reflection" and those measured in "transmission," suggesting high effective absorption in the interior of the crystal.

A second check for the absence of extinction effects was obtained directly from the ratios of the intensities of the measured magnetic reflections. For each magnetic reflection, the integrated intensity $I(hkl)$ is proportional to

$$\frac{A_c f^2 e^{-2W}(T_c-T)^{2\beta}}{\sin 2\theta}, \tag{5}$$

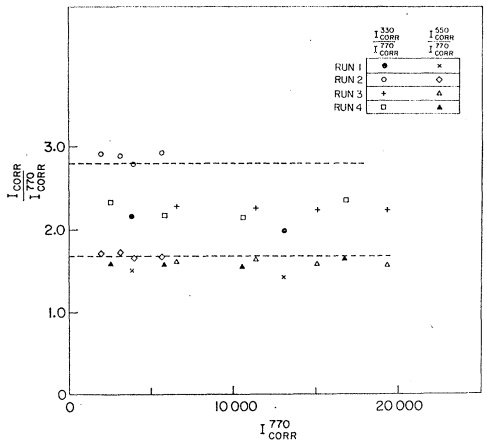

FIG. 6. Variation of observed magnetic intensity ratios $I(330)/I(770)$ and $I(550)/I(770)$ with increasing (770) intensity, i.e., decreasing temperature. The calculated ratios are 2.8 and 1.7, respectively, and are indicated by the dashed lines in the figure.

since the magnetic structure factor is the same for all three peaks. In the above equation A_c is the absorption constant, f is the magnetic form factor, e^{-2W} is the Debye-Waller factor, and sin 2θ is the Lorentz factor. In the absence of extinction the ratios $I(330)/I(770)$ and $I(550)/I(770)$ should thus be independent of the temperature and equal to the values calculated from Eq. (5): 2.8 and 1.7, respectively. If extinction were present, these ratios would decrease as the temperature decreases, i.e., as $I(770)$ increases. A plot of these ratios against $I(770)$ is shown in Fig. 6. The ratios show discrepancies from the calculated values similar to those observed for the nuclear intensity ratios and are not fully understood. However, it is clear that there is no trend with intensity, showing that the value of β should not be affected by extinction. As a further check, β was evaluated separately for each of the three reflections. As will be seen in Sec. V, the value of β is the same for all three.

V. DATA ANALYSIS

The magnetic peak intensities were fitted to the power-law expression, Eq. (1), by least-squares procedures. As described in Sec. IV, the fitting was complicated by the existence of different normalization constants for each run as well as for each of the magnetic reflections. The equation to be fitted is

$$I_{\text{corr}\ i}{}^{h}=A_i{}^{h}(T_c-T)^{2\beta}, \tag{6}$$

where $I_{\text{corr}}=I_T-B_{\text{cs}}$; $h=3$, 5, or 7 for the (330), (550), or (770) reflections; and i designates one of the four runs. Table III shows the magnetic intensities with the multiple-Bragg peaks and critical scattering background subtracted, as well as the ratios of critical scattering intensities to the correct intensities. Since the value of β was closely coupled to the value of T_c, T_c was treated as an unknown parameter in the fits. The weighting of the points in the least-squares fit was determined from the standard deviation of the intensities plus a term representing the uncertainty in the background, i.e.,

$$\epsilon=\sqrt{I_T+\tfrac{1}{2}B_{\text{cs}}}. \tag{7}$$

These errors are listed in Table III.

The temperature dependence of the magnetization was first fitted for each reflection separately. For each reflection, four values of $A_i{}^{h}$ and one β had to be determined for each choice of T_c. T_c could have been included in the fit, but it was important to see explicitly how β varied with the choice of T_c. Figure 7(a) shows both the standard deviation of the fit, σ^2, and the value of β as a function of the choice of T_c for each of the three peaks. On the β curves, the circles represent the best fit and the solid lines represent the 90% confidence level. The fit for T_c is shallow on the high-temperature side, but all three fits predict almost the same T_c, about 2.5175°K. At this T_c, β for the (770) is about 0.275, while the value for the (330) and (550) peaks is about 0.26. The least-squares errors on β were about 0.006, but consideration of errors due to the uncertainty in T_c and the weighting of the points makes 0.02 a more realistic error. There is no consistent trend in the values of β for the three peaks to indicate extinction. Figure 8 shows the least-squares fit for

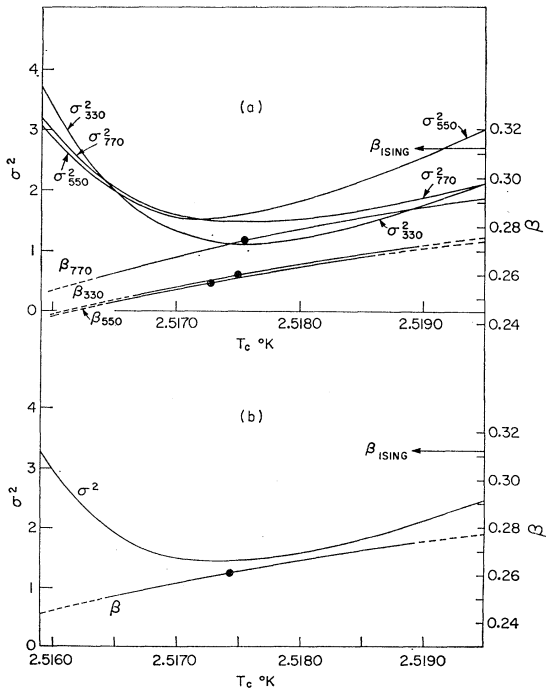

FIG. 7. Critical exponent β and standard deviation σ^2 of the fit to the power law as a function of T_c. In (a) the data for each magnetic peak were treated separately in the least-squares analysis, whereas in (b) the data for all three peaks were fitted simultaneously.

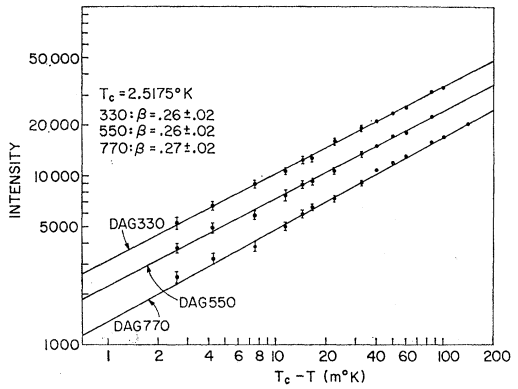

FIG. 8. Log-log plot showing results of least-squares determinations of β for individual magnetic reflections and for the best value of T_c, 2.5175°K.

$T_c=2.5175$°K, where the normalization constants have been adjusted so that the four runs for a given ($hh0$) can be plotted on one line.

In addition, the temperature dependence of the magnetization was also fitted for all ($hh0$) peaks simultaneously. In this fit, there were 12 values of $A_i{}^h$ and one β to be found as a function of T_c with 42 data points. Figure 7(b) shows β and σ^2 as a function of T_c, as before. The best fit occurs for $T_c=2.5175$°K as before, and the β value of 0.26 is consistent with the ones obtained above. The 12 $A_i{}^h$ values for this fit are given in Table III. Figure 9 shows the results of this fit for $T_c=2.5175$°K where the A's have been normalized so all runs and reflections can be compared on the same basis. For clarity, the relative positions of points on the graph are indicated by the sequence of numbers (h values) adjacent to the line.

At the suggestion of Fisher, an attempt was made to fit the data to the expression

$$I_{\text{corr}}=A\left(\frac{T_c-T}{T_c}\right)^{2\beta}\left[1-2b_F\left(\frac{T_c-T}{T_c}\right)\right], \qquad (8)$$

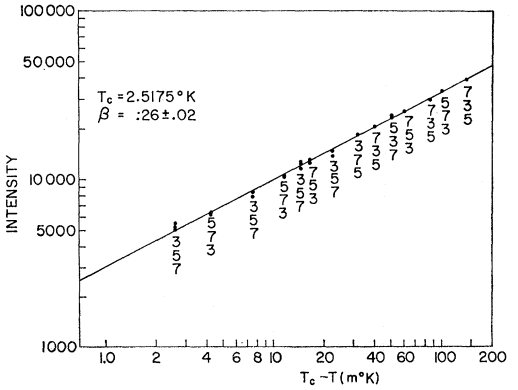

FIG. 9. Log-log plot illustrating the determination of β by least-squares treatment of all three peaks simultaneously. The sequence of integers adjacent to the line at a given temperature indicates the relative positions of the points corresponding to the three Bragg peaks. The best values of β and T_c are 0.26±0.02 and 2.5175°K.

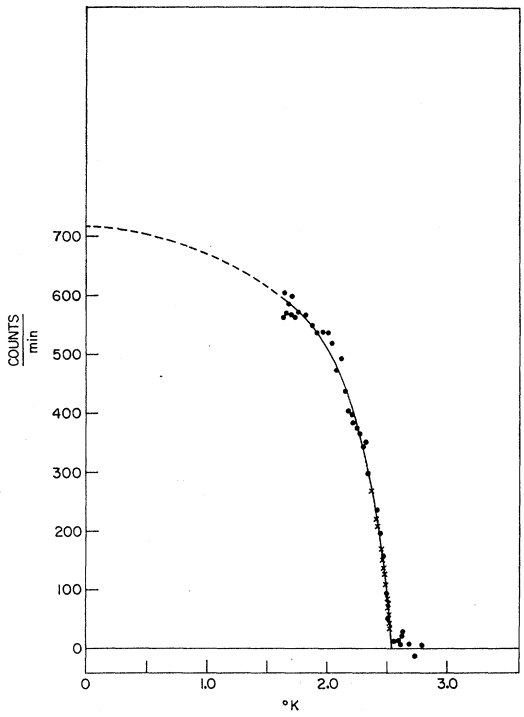

FIG. 10. Sublattice magnetization of DAG as a function of temperature. The circles and solid curve represent the powder diffraction data of Herpin and Mériel (Ref. 21) and the dashed curve is their extrapolation to 0°K. The crosses represent the (330) data of the present study scaled to the powder data.

which represents the first-order correction to the power law. The implication here is that the simple power law had perhaps already begun to fail in the measured temperature range, and that the above expression might fit the data better and lead to a higher value of β. Using a value of $b_F=0.83$ calculated for a three-dimensional bcc Ising model,[25] the value of β was found to be 0.285 and $T_c=2.5184$°K. No significant improvement of the fit was found. However, as will be discussed in II the critical scattering data make such a high value of T_c unlikely. For a value of $T_c=2.5172$°K, as obtained from the critical scattering, the best value of β is 0.28, but the fit to Eq. (8) is significantly worse than for the case $b_F=0$.

In addition to predicting the critical exponent, the theories also predict the constant D, which is defined by

$$\frac{M(T)}{M(T=0)}=D\left(\frac{T_c-T}{T_c}\right)^{\beta}. \qquad (9)$$

Essam and Fisher[4] found D to have the values 1.570 ±0.001, 1.491±0.001, and 1.488±0.001 for simple cubic, bcc, and fcc Ising models, respectively, and Baker and Gaunt[5] found $D=1.661\pm0.001$ for the diamond lattice. An estimate of D was obtained by combining our measurements with those of Herpin

[25] M. E. Fisher (private communication).

and Mériel.[21] They measured the magnetization of a DAG powder sample (for which extinction is absent) down to 1.6°K and were able to extrapolate to $T=0$. Their measurements and extrapolated curve are shown in Fig. 10. Our magnetization measurements were scaled to their data by finding the proper multiplicative factor and are also shown in Fig. 10. The agreement is quite good. Using their extrapolated value of the magnetic Bragg intensity at $T=0$, the multiplicative scaling factor, and our value of β, we find $D=1.3\pm0.1$, where the error includes the uncertainties in all the quantities other than the extrapolation. If we allow for the possibility of a somewhat lower extrapolation, a value of D as high as 1.5 cannot be ruled out completely. In any case the range of possible values is in good agreement with the range of values calculated for different cubic lattices, and until a calculated value for the specific garnet lattice becomes available a more detailed comparison is not worthwhile.

VI. CONCLUSIONS

Measurements of the spontaneous magnetization give $\beta=0.26\pm0.02$. The most likely value of T_c is 2.5175°K on a relative temperature scale, with an uncertainty in absolute temperature of about 10 m°K. While higher values of β are not inconsistent with the magnetization measurements, such values would require increases in T_c which are incompatible with the critical scattering above T_c (see discussion in II). The existence of such a low value of β is somewhat surprising. Inasmuch as DAG deviates from a simple Ising model by the addition of finite long-range dipolar forces, one might perhaps have expected a value of β falling somewhere between the Ising prediction, 0.312, and the mean-field value, 0.5. Such a shift in a critical exponent has previously been found by Joyce,[26] who computed γ for a two-dimensional Ising model with a long-range potential proportional to $1/r^3$. However, it is clear that the actual situation in DAG is far more complex with interactions of different signs as well as varying strengths, and it would appear from our results that such a combination can in fact lead to a β value outside the range covered by the Ising and mean-fields models. On the other hand, results for the two other critical exponents, γ and ν, which can be measured by neutron scattering (see II) give values which do lie between the mean-field and nearest-neighbor Ising predictions, and we can only conclude that further theoretical studies are needed for systems with other than purely nearest-neighbor forces. Detailed calculations for real systems such as DAG would appear to be prohibitively difficult and one must hope that some general theoretical guide lines will be evolved for understanding the critical exponents in more complex systems.

ACKNOWLEDGMENTS

We wish to thank Professor M. E. Fisher for several helpful discussions. One of us (WPW) would also like to thank the Physics Department of the Technische Hochschule, Munich, for their hospitality during the preparation of parts of this manuscript.

[26] G. S. Joyce, Phys. Rev. **146**, 349 (1966).